Heterogeneous Azeotropic Distillation: Experimental and Simulation Results

Experimental measurements for an industrial azeotropic distillation tower that dehydrates secondary butyl alcohol (SBA) show erratic operation that only approaches a steady state. These are explained with steady-state simulations which show that slight variations in the aqueous reflux rate cause many trays to shift from homogeneous to heterogeneous operation, accompanied by significant changes in the SBA purity, with water or entrainer contaminating the bottoms product. When other methods failed, an arc-length homotopy-continuation method made small adjustments in the reflux ratios to obtain close agreement with the measurements.

J. W. Kovach III and W. D. Seider
Department of Chemical Engineering
University of Pennsylvania
Philadelphia, PA 19104

Introduction

Azeotropic distillation is commonly used to separate close boiling mixtures with far fewer trays than in conventional distillation and with less recirculation, resulting in lower equipment and energy costs. It is widely used for the dehydration of alcohols and is being applied in new areas of chemical processing because of its efficiency.

In a typical configuration for the dehydration of an alcohol, Figure 1, one or more towers concentrate the dilute alcohol to compositions approaching the alcohol-water azeotrope. The resulting stream is fed to the azeotropic tower along with an entrainer-rich reflux stream. A pure alcohol stream is withdrawn from the bottom of the azeotropic tower, and an overhead stream that condenses into two liquid phases is sent to a decanter. The aqueous phase from the decanter is fed to the top tray of a stripping tower, where most of the water in the feed to the azeotropic tower is recovered in high purity. The overhead vapor, containing alcohol, water, and entrainer, is condensed and recycled to the decanter. A small makeup stream of entrainer is necessary to replace small losses in the alcohol and water product streams.

Because of the nonideality of azeotropic systems, azeotropic distillation is characterized by steep fronts in both the temperature and concentration profiles. Robinson and Gilliland (1950) were the first to calculate these profiles, and an extensive literature has since developed. The great sensitivity of the steep fronts to small changes in the operating conditions, such as the reflux ratio and the boilup rate, make it extremely difficult to identify specifications that permit a realistic solution to the MESH (Material balance, Equilibrium, Summation of mole fractions, and Heat balance) equations. This problem which was addressed by Prokopakis and Seider (1983a) becomes more difficult to resolve when two liquid phases occur on the trays (Ross and Seider, 1980; Schuil, 1984). In addition, the equations are sufficiently complex to admit regions of the parameter space in which two or more steady-state solutions exist (Magnussen et al., 1979; Prokopakis et al., 1981; Prokopakis and Seider, 1983a and b). Thus far, the problems of sensitivity to specifications, heterogeneous trays, multiple steady-state solutions, and algorithm reliability have not been addressed in a unified way. Our work has been addressing these problems (Kovach, 1986), but the volume and scope of this source is too extensive to appear in any one journal article. The present paper introduces a more rigorous model and solutions, using a new algorithm (Kovach and Seider, 1987b) that could not be obtained with the previous algorithms. These solutions explain the observations of several researchers whose results were, until now, difficult to reconcile. Furthermore, and perhaps most important, these solutions are confirmed by experimental data which, to our knowledge, are the first to appear in the literature. The data were taken using an ARCO tower that dehydrates secondary butyl alcohol (SBA) in a methyl ethyl ketone (MEK) plant.

Commercially, methyl ethyl ketone is prepared by the catalytic dehydrogenation of secondary byutl alcohol, which is formed by hydrating butyl sulfates. A process flowsheet that traces the conversion of mixed butylenes to SBA in the production of MEK is presented in Figure 2. Sulfuric acid is reacted with cis- and trans-2-butene to create butyl sulfates which are hydrated to produce SBA. The reaction mixture is steam stripped and scrubbed with caustic to remove sulfuric acid, flashed to remove unreacted butylenes, and sent to the SBA I

J. W. Kovach III is currently with Shell Development Company, Houston, TX.

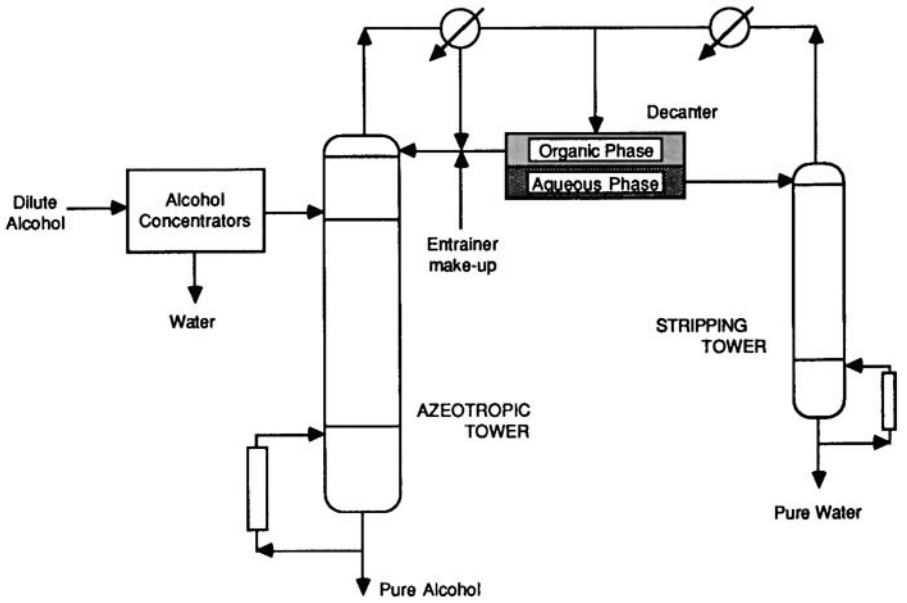

Figure 1. Typical configuration for dehydration of alcohol.

distillation tower (10 trays, approx. 2 bar) to remove heavy oils and to bring the SBA-water mixture close to its azeotropic composition (approximately 40 mol % SBA). The distillate is mixed with a recycle stream from the MEK reaction section and fed to the SBA II tower; representative feed compositions are shown in Table 1. Note that this stream forms two liquid phases and contains the reaction by-product, di-secondary butyl ether (DSBE), which is the entrainer in the SBA II tower. This 41-tray azeotropic tower produces a nearly pure SBA bottoms product and an overhead vapor that condenses to form aqueous and organic phases, Table 1. The aqueous phase is recycled to the acid stripping operation. The organic phase is washed with water to recover DSBE and SBA and sent to product storage. The bottoms product from the SBA II tower (99+ wt. % SBA) is sent to the SBA III tower (45 trays, approx. 2 bar) where any remaining heavy by-products are removed. The overhead from the SBA III tower is sent to the MEK reactors.

SBA II Distillation Tower

A process instrumentation diagram (PID) for the SBA II tower is presented in Figure 3. The tower has 40 sieve trays, a 1.981 m ID, and measures 25.1 m tangent-to-tangent. Its tray spacing varies from 0.41 to 0.61 m and it is equipped with a decanter that provides a 40 to 50 min residence time for the combined aqueous and organic phases. Residence times for the

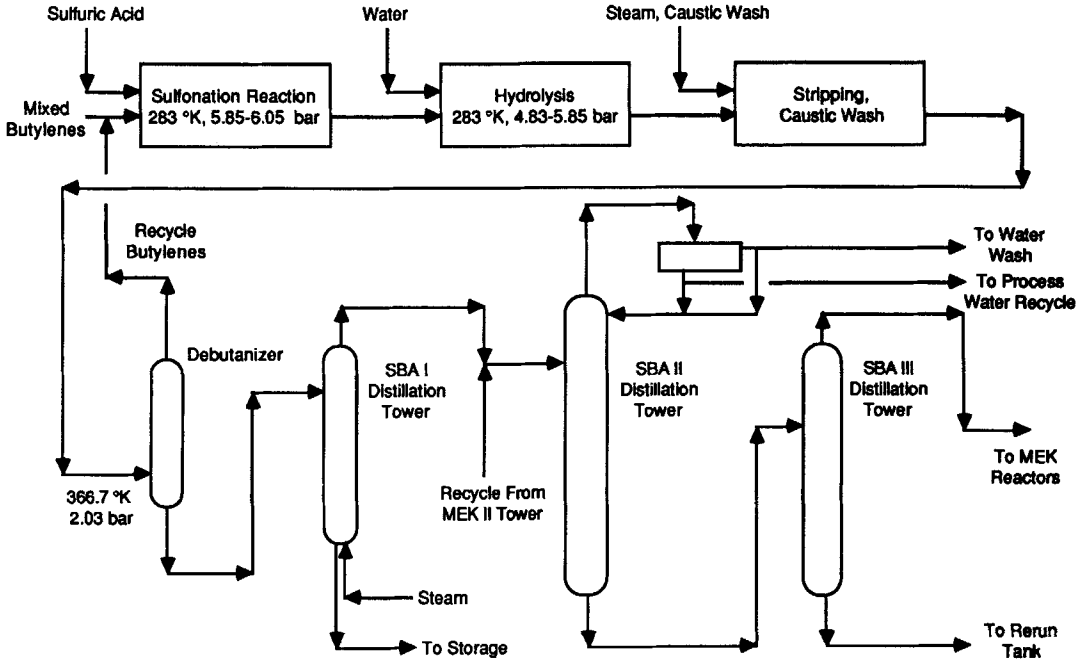

Figure 2. Butylene to SBA in production of MEK.

Table 1. Stream Composition Data* for SBA II Tower, 10/25/84–11/5/84

	Feed	Bottoms	Organic Reflux	Aqueous Reflux**
			Mole Percent	
SBA	41.0	96.9	40.1	2.7
DSBE	0.9	0.5	30.7	<<0.1
Water	57.4	2.0	17.8	96.6
MEK	0.2	0.6	2.3	0.2
Butylenes	0.5	0.0	9.0	0.5
Total	100.0	100.0	99.0	100.0
			Range	
SBA	41.0–44.0	83.1–98.7	41.9–45.2	2.5–3.3
DSBE	0.7–2.0	0.3–5.6	23.3–31.5	0.0–0.0
Water	53.6–58.0	0.4–16.5	20.8–23.3	97.3–96.1
MEK	0.1–0.3	0.0–0.1	2.1–3.8	0.1–0.2
Butylenes	0.5–0.6	—	0.4–7.6	0.3–0.5

*Stream analysis by gas chromatograph, water by Karl-Fischer analysis
**Aqueous phase composition available for test date 11/6/84 only

aqueous and organic phases are approximately 4 h and 20 min, respectively. Heat is supplied by a 175.1 m^2 thermo-siphon reboiler and is removed in a 319.6 m^2 condenser. The temperatures of tray 31 and the bottoms stream are recorded using strip charts, while temperature indicators are used for tray 36 and the overhead vapor and the reflux streams. Overhead and bottoms pressures are read from gauges mounted on the tower. The feed, organic product, aqueous reflux, and steam rates are under flow rate (recorder) control. The bottoms flow rate is adjusted by level control and is measured by a gauge located downstream of the control valve. The aqueous product rate and organic reflux rate are adjusted by level control in the phase separator and monitored by flow recorders. Although details of the calibration of the flow gauges were unavailable, the mass balances closed to within 5% and the flow rates were in close agreement with the theoretical results (to be presented).

Under normal operating conditions, the feed rate and reboiler stream rates are nearly steady, while the aqueous and organic reflux rates and T_{31} fluctuate. Typical, near steady, operating conditions are shown in Figure 4. The subcooled two-phase feed enters the tower on tray 10. The overhead stream, which has a composition close to that of the SBA/DSBE/water azeotrope, is condensed to form two liquid phases, subcooled to 305–315 K, and sent to the decanter. Most of the organic phase, but only a small amount of the aqueous phase, is refluxed to the tower.

In normal operation, the operator adjusts the aqueous reflux rate to position the temperature front between trays 31 and 36. This front indicates a significant change in composition and is closely monitored to keep the bottoms product on specification. When positioned between trays 31 and 36, the bottoms product is 99% pure, with a 90% recovery of SBA. Usually, the aqueous product flow rate is relatively steady, with oscillations of ±6% occurring over a 1 min period, on the average. However, after disturbances, the level controller in the decanter may vary the flow rate by 10 to 30%.

Strip chart recordings and log sheets for two weeks, from Oct. 26 to Nov. 5, 1984, help to describe the operation of the tower during periods with few disturbances. Data for the days during which the tower produced off-specification product are presented in Table 2 and will be discussed later.

Dynamics Test

The dynamics test was initiated at 0810 hours on Nov. 6, 1984, with a 13% decrease in the feed flow rate. This was fol-

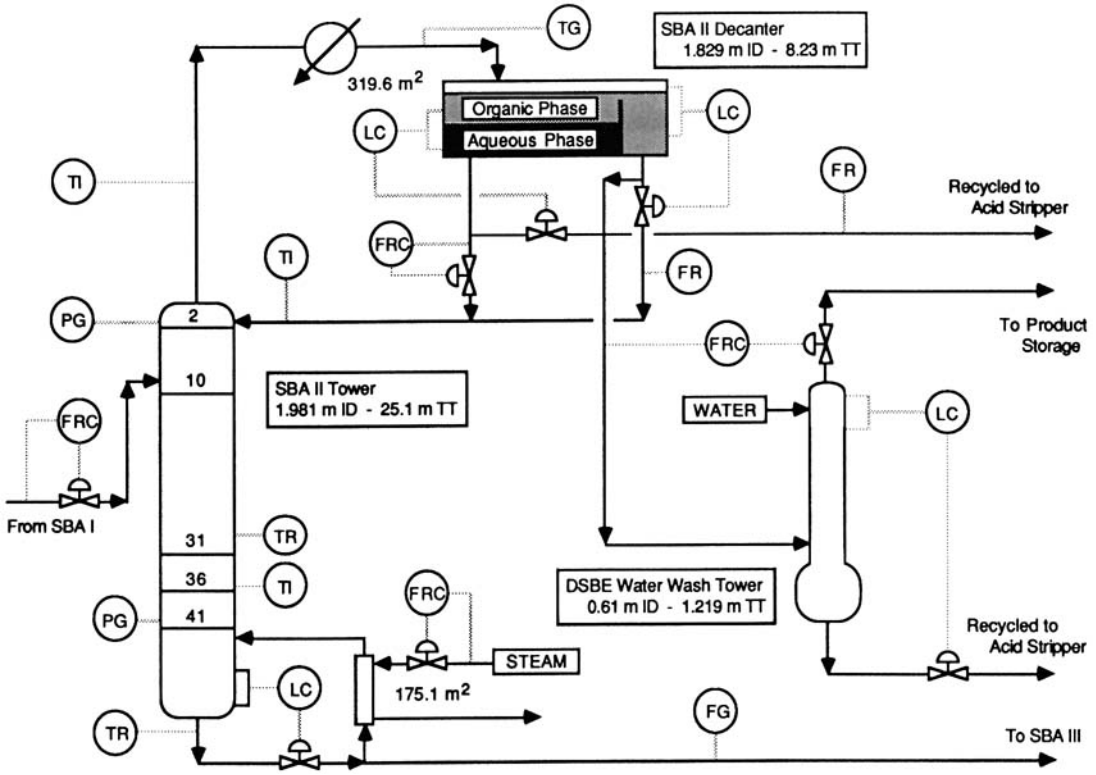

Figure 3. PID for SBA II distillation tower.

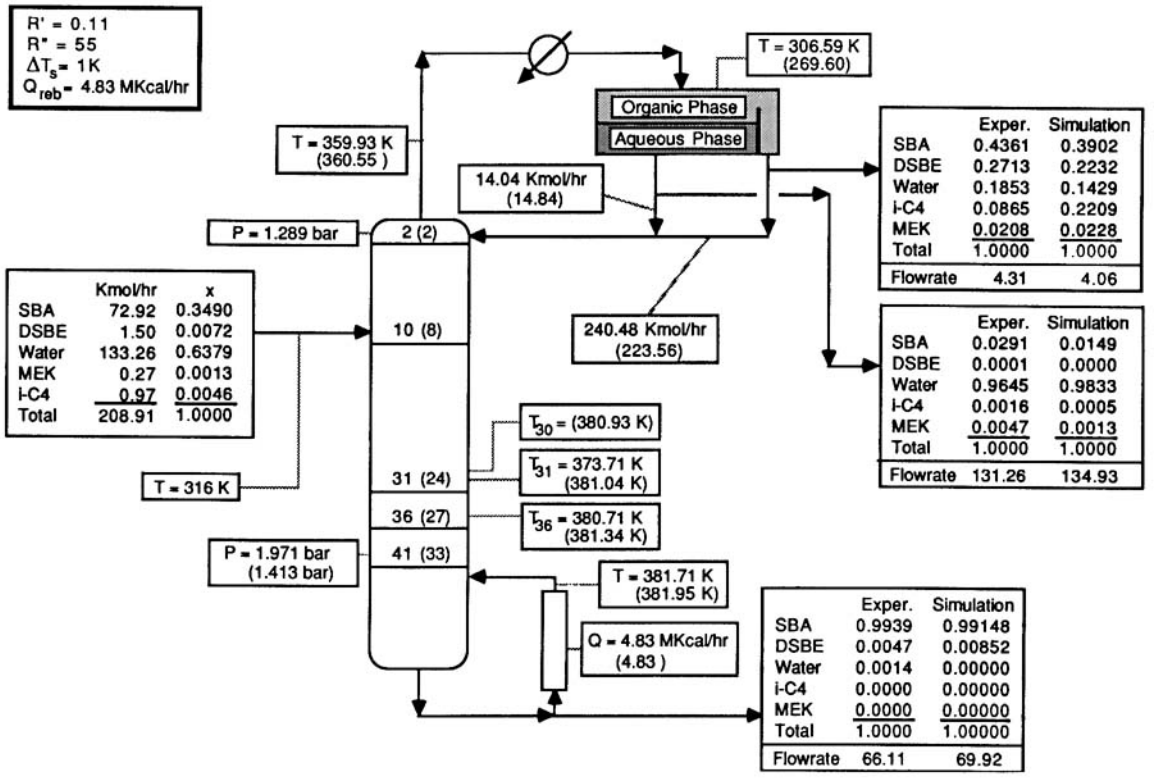

Figure 4. Comparison of initial simulation results (in parentheses) with experimental data.

lowed by a 13% increase at 1153 hours. Feed samples were taken at 0800, 1000, and 1600 hours, while bottoms, aqueous, and organic reflux samples were taken at 15 min to 1 h intervals. Temperature indicators for the overhead, decanter, reflux, bottoms, and tray 36 were read at 10 to 30 min intervals. The bottoms flow rate was measured at the same time intervals. The process stream samples were analyzed by gas chromatograph and Karl-Fischer titration at an on-site laboratory.

To hold the temperature front stationary when the feed rate was changed, the operator tried to keep the total amount of water entering the tower constant. By decreasing the feed, the water entering the tower was decreased, and the aqueous reflux was increased to compensate. Conversely, when the feed was increased, the aqueous reflux was decreased. This operator control strategy is, in general, effective, but does not lead to a steady temperature on tray 31.

Model

To trace the real-time response to changes in the feed and aqueous reflux flow rates, a dynamic model is desirable. In this work, however, a steady-state model was implemented to give the limiting solutions before extending the model to perform dynamic simulations.

The notation used in this paper is that of Napthali and Sandholm (1971). The tower is modeled as a combination of models for the standard trays, a reboiler, and a condenser/decanter (phase separator). We have implemented a very general model (Kovach, 1986), which is briefly summarized in the next paragraph. The equations and figures that follow, however, include only those terms used to simulate the SBA II tower.

Consider a column having N_t stages and separating N_s species that may form one or two liquid phases. The top stage is referred to as tray 1 and is modeled as a standard tray (e.g., to represent a partial condenser with a specified heat duty) or a condenser/decanter. The bottom stage, tray N_t, may be modeled as a standard tray (e.g., as in a steam stripper) or a reboiler. Vapor or liquid streams may be exchanged between nonadjacent stages. There may be occlusion of the vapor in the liquid stream, entrainment of the liquid in the vapor stream, and chemical reaction occurring in the liquid on the trays. A separate Murphree tray efficiency may be specified for each species. However, when two liquid phases exist, they are modeled in equilibrium. A feed stream may be introduced on each tray. Also, vapor or liquid side streams may be withdrawn from each tray. The intermediate stages may have a specified heat duty.

The representation of tray i in Figure 5 illustrates the variables in the mass and energy balances that follow. Note that the Murphree tray efficiencies and variables associated with vapor occlusion, liquid entrainment, flow between nonadjacent trays, and chemical reaction have been omitted. These are incorporated in our HOMDIS program, with the full model presented by Kovach (1986). v_{ji}, T_i, and l_{ji} are respectively the flow rate of species j in the vapor leaving tray i (after the sidedraw is removed), the temperature, and the flow rate of species j in the liquid. These are usually unknown and are the iteration variables of the Napthali-Sandholm model. When necessary, the flow rates of species j in the second liquid phase, l''_{ji}, are introduced, and a superscript prime is added for the first liquid phase (i.e., l'_{ji}). The total flow rates for the three phases are V_i, L'_i, and L''_i. The mass balances for species j on tray i are:

Table 2. Operating Data that Accompany Off-specification Product

		Date, Hour			
	Normal	10/26 0500	10/29 1700	10/30 0500	11/2 0500
			Bottoms		
SBA	0.9948	0.8312	0.9387	0.9544	0.8548
DSBE	0.0043	0.0035	0.0559	0.0281	0.0046
Water	0.0009	0.1653	0.0043	0.0165	0.1397
MEK	—	—	0.0011	0.0010	0.0009
i-C4	—	—	—	—	—
Total	1.0000	1.0000	1.0000	1.0000	1.0000
			Organic Reflux		
SBA	0.4195	0.4518	N.A.	0.4424	0.4354
DSBE	0.3154	0.2328	N.A.	0.2461	0.2709
Water	0.2222	0.2167	N.A.	0.2300	0.2080
MEK	0.0384	0.0225	N.A.	0.0258	0.0213
i-C4	0.0045	0.0762	N.A.	0.0557	0.0644
Total	1.0000	1.0000	N.A.	1.0000	1.0000
			Feed		
SBA	0.4198	N.A.	N.A.	0.4399	N.A.
DSBE	0.0089	N.A.	N.A.	0.0156	N.A.
Water	0.5641	N.A.	N.A.	0.5356	N.A.
MEK	0.0018	N.A.	N.A.	0.0025	N.A.
i-C4	0.0054	N.A.	N.A.	0.0064	N.A.
Total	1.0000	N.A.	N.A.	1.0000	N.A.
Flow Rate, gpm					
Feed	41	39.6	20.4	28.2	31.2
Aqueous reflux	3	2.5	3.4	4.1	3.8
Organic reflux	110	108	98.3	99	99
Aqueous overhead	10	11.4	9.0	8.4	8.2
Organic overhead	2	1.3	1.5	1.7	1.2
Bottoms	28	27.0	8.5	18.0	20.2
Temperature, K					
Reflux	317.6	319.8	313.2	318.2	309.8
Tray 31	374.8	378.2	365.9	378.7	375.2–378.2
Bottoms	383.2	383.2	382.6	383.2	380.9
Bottoms Pressure, bar					
Measured	1.971	2.047	1.964	1.978	1.910
Calculated	1.413	1.897	1.474	1.535	1.709
Difference	0.558	0.150	0.490	0.443	0.201
Steam Rate, Mkcal/h	4.76	5.03	4.42	4.42	4.08

N.A., not available
Aqueous reflux compositions not available
SI conversion: L/s = gpm × 0.0631

$$M_{ji} = (1 + S_i^V)v_{ji} + (1 + S_i')l_{ji}' + (1 + S_i'')l_{ji}'' + y_{ji}A_i^V + x_{ji}'A_i' + x_{ji}''A_{ji}'' - v_{j,i+1} - l_{j,i-1}' - l_{j,i-1}'' - f_{ji}^V - f_{ji}^L = 0 \quad j = 1, \ldots, N_s \quad (1)$$

The energy balance is:

$$E_i = (1 + S_i^V)V_iH_i + (1 + S_i')L_i'h_i' + (1 + S_i'')L_i''h_i'' + A_i^VH_i + A_i'h_i' + A_i''h_i'' - V_{i+1}H_{i+1} - L_{i-1}'h_{i-1}' - L_{i-1}''h_{i-1}'' - F_i^VH_i^F - F_i^Lh_i^F + Q_i = 0 \quad (2)$$

The equations for vapor-liquid equilibrium, with a Murphree tray efficiency equal to unity, are:

$$Q_{ji}^{VL} = \frac{K_{ji}V_il_{ji}'}{L_i'} - v_{ji} = 0 \quad j = 1, \ldots, N_s \quad (3)$$

Finally, the equation for liquid-liquid equilibrium is:

$$Q_{ji}^{LL} = \frac{l_{ji}'}{L_i'}\gamma_{ji}' - \frac{l_{ji}''}{L_i''}\gamma_{ji}'' = 0 \quad j = 1, \ldots, N_s \quad (4)$$

The variables A_i^V, A_i', and A_i'' permit the specification of "absolute" flow rates of the side streams. Note that Eqs. 4 are included only when a second liquid phase exists on tray i. With just one liquid phase, these equations are dropped and l_{ji}'' are eliminated from the remaining equations.

Equations 1–4 apply to the interior trays of the column as well as a partial condenser and reboiler when the heat duty is known. There are $NP_iN_s + 1$ equations with $NP_iN_s + 1$ unknowns for each tray, where NP_i is the number of phases on tray i. Using the ordering of Wayburn and Seader (1984), the material balances are the first N_s equations, the energy balance is the $N_s + 1$ equation, and the equilibrium equations follow. Furthermore, v_{ji} are

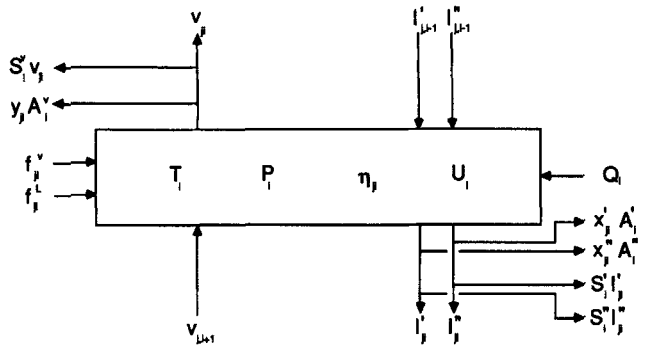

Figure 5. Schematic of tray *i*.

tion, and the equilibrium equations follow. Furthermore, v_{ji} are the first N_s unknown variables, followed by T_i, l'_{ji}, and l''_{ji} (when applicable). The vectors of functions and iteration variables are:

$$\underline{f}_i = [M_{1,i} \ldots M_{N_s,i} E_i Q^{VL}_{1,i} \ldots Q^{VL}_{N_s,i} Q^{LL}_{1,i} \ldots Q^{LL}_{N_s,i}]^T$$

$$\underline{x}_i = [v_{1,i} \ldots v_{N_s,i} T_i l'_{1,i} \ldots l'_{N_s,i} l''_{1,j} \ldots l''_{N_s,i}]^T$$

These place the large temperature derivative of the energy balance on the diagonal and reduce the need for pivoting during the inversion of the $\underline{\underline{B}}$ submatrix of the Jacobian, Figures 6 and 7.

For the reboiler, the energy balance is replaced with a specification equation. The specifications may include the bottoms flow rate of an individual species, the total bottoms flow rate, the boilup rate (total or species), boilup ratios, and purity. Specifications involving the flow rates of the liquid phase refer to the combination of both liquid phases (e.g., the specification of the purity refers to the average liquid mole fraction).

With the exception of the mass balance and liquid-liquid equilibrium equations, the equations describing the condenser/decanter differ significantly from those for a standard tray. Consider first the diagram in Figure 8, with the key variables annotated. The mass balances are:

$$M_{j1} = (1 + S'_1) l'_{j1} + (1 + S''_1) l''_{j1} + d'_j + d''_j + x'_{j1} A'_1 + x''_{j1} A''_1 - v_{j,2} - f^L_{j1} - f^V_{j1} = 0 \quad j = 1, \ldots, N_S \quad (5)$$

Note that the variables $\underline{d}'$, $\underline{d}''$, A'_1, A''_1, and S'_1, S''_1 permit alternate specifications for the two distillate liquids. The energy balance is replaced by a specification equation,

$$SP1 = \text{spec}_1 - f\{\underline{d}', \underline{d}'', T_1, \underline{l}'_1, \underline{l}''_1\} \quad (6)$$

where the function permits several specifications including T_1 and the reflux ratios, $R' = \Sigma l'_j / \Sigma d'_j$ and $R'' = \Sigma l''_j / \Sigma d''_j$. The equations for vapor-liquid equilibrium, Eqs. 5, are replaced by the bubble point equation:

$$BP_1 = 1 - \Sigma x'_{j1} K_{j1}\{T_1 + \Delta T_s, \underline{x}'_1\} = 0 \quad (7)$$

where ΔT_s are the degrees of subcooling, and composition equalities:

$$EQ'_{j1} = \frac{l'_{j1}}{\sum_k l'_{k1}} - \frac{d'_j}{\sum_k d'_k} = 0 \quad j = 1, \ldots, N_S - 1 \quad (8)$$

Note that in Eq. 8 only $N_s - 1$ equations are independent. Hence, the equation associated with the species in the lowest concentration is excluded. Finally, Eq. 4 is modified to express the equilibrium between the two liquid phases:

$$Q^{LL}_{j1} = x'_{j1} \gamma'_{j1}\{T_1 + \Delta T_s, \underline{x}'_1\} - x''_{j1} \gamma''_{j1}\{T_1 + \Delta T_s, \underline{x}''_1\} \quad j = 1, \ldots, N_s \quad (9)$$

and used with a specification equation:

$$SP2 = \text{spec}_2 - f\{\underline{d}', \underline{d}'', T_1, \underline{l}'_1, \underline{l}''_1\} \quad (10)$$

and the composition equalities:

$$EQ''_{j1} = \frac{l''_{j1}}{\sum_k l''_{k1}} - \frac{d''_j}{\sum_k d''_k} = 0 \quad j = 1, \ldots, N_S - 1 \quad (11)$$

When the vapor condenses into just one liquid phase, the decanter is not needed and Eqs. 9–11 are excluded.

The mass balance Eqs. 5 are similar to those of a standard tray, but are expressed in terms of $\underline{d}'$ and $\underline{d}''$ rather than $\underline{v}_1$. When the decanter temperature is specified below saturation, the bubble point equation is removed and T_1 is removed from the iteration variables. The functions in Eqs. 6 and 11 allow many specifications, a few of which are:

1. The distillate flow rate of one species in either phase
2. The total distillate flow rate of both phases
3. The average mole fraction of a species in the decanter
4. The ratio of the reflux ratios, R'/R''

If necessary, the functions can be modified to include new specifications.

There are $NP_1N_s + 1 + (NP_1 - 2)N_s$ equations in $NP_1N_s + 1 + (NP_1 - 2)N_s$ unknowns for the condenser/decanter, with the number reduced to $2N_s + 1$ when the decanter is not necessary. The vectors of functions and iteration variables are:

$$\underline{f}_1 = [M_{1,1} \ldots M_{N_s,1} SP1\, BP_1 EQ'_{1,1} \ldots EQ'_{N_s-1,1} Q^{LL}_{1,1} \ldots Q^{LL}_{N_s,1} SP2\, EQ''_{1,1} \ldots EQ''_{N_s-1,1}]^T$$

$$\underline{x}_1 = [d_{1,1} \ldots d_{N_s,1} T_1 l'_{1,1} \ldots l'_{N_s,1} l''_{1,1} \ldots l''_{N_s,1} d''_{1,1} \ldots d''_{N_s,1}]^T$$

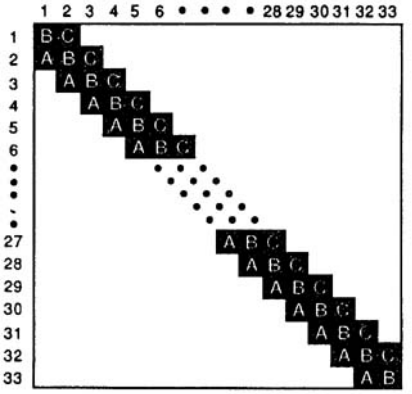

Figure 6. Block tridiagonal structure of Jacobian matrix.

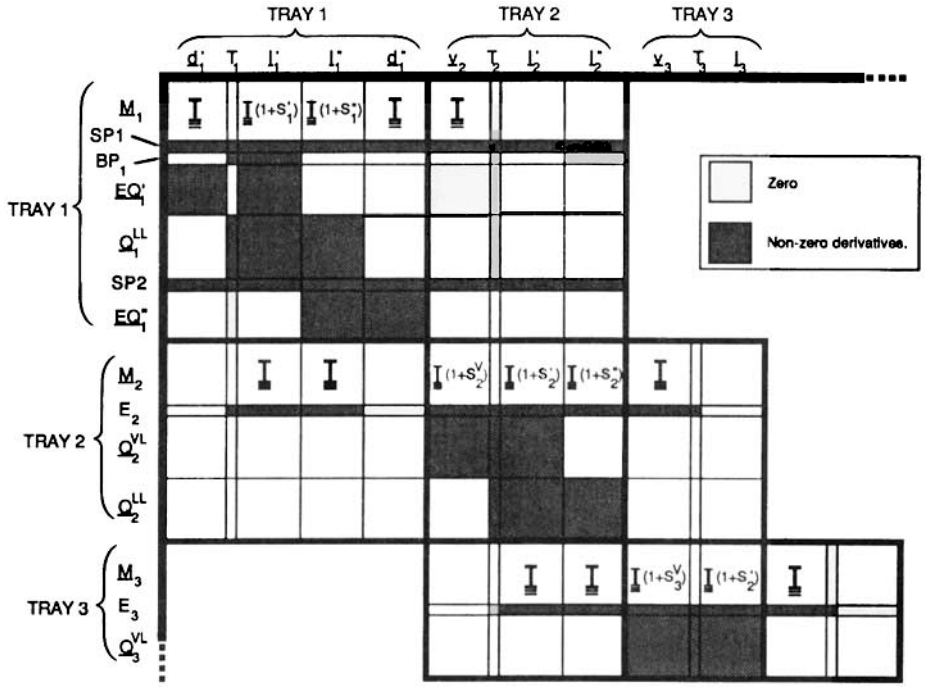

Figure 7. Sparsity pattern for a decanter and two standard trays.
Trays 2 and 3 have two and one liquid phases, respectively.

The specifications for the tower include the tray pressures, tray heat duties, and the location of the side streams, and feed streams. The condenser/decanter and reboiler specification functions are each restricted to variables present in the condenser/decanter and reboiler, respectively. When alternate specifications such as the flow rate on an intermediate tray or two mole fractions in the reboiler are required, the approach of Ferraris and Morbidelli (1982) can be followed by adding an equation and variable. It allows for very flexible specifications and could easily be added to our model.

The equations and variables are grouped according to stage to produce the block tridiagonal Jacobian matrix in Figure 6. Figure 7 shows the pattern of the derivatives for a condenser/decanter and two standard trays with three, three, and two phases, respectively. The vapor phase is modeled by an equation of state and the liquid phase by the product of the pure liquid fugacity and the activity coefficient (currently computed using the UNIQUAC and NRTL equations). All derivatives are evaluated analytically and are presented by Kovach (1986).

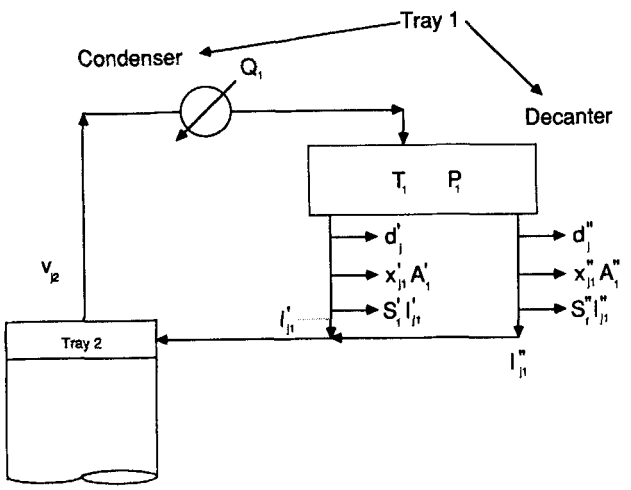

Figure 8. Schematics of condenser/decanter.

Simulation Results

The results are reported for a tower with 33 ideal trays, including a condenser/decanter and a reboiler, and assuming an overall efficiency of 80%. The feed is subcooled to 316.48 K and introduced on tray 8, which corresponds to tray 10 in the experimental tower. The heat capacity coefficients and enthalpies at 298 K are presented in Tables 3 and 4. The vapor phase is assumed to be ideal. The vapor pressures are modeled using the extended Antoine equation, with coefficients shown in Table 5, and the liquid phase activity coefficients modeled using the modified UNIQUAC equation with the structural parameters and interaction coefficients shown in Table 6. Vapor-liquid and liquid-liquid equilibrium data were measured for the SBA-DSBE-water system and the q-prime parameters and interaction coefficients determined by regression (Kovach and Seider, 1987a). The remaining interaction coefficients were calculated by the CHEMTRAN program (ChemShare Corporation), using infinite dilution activity coefficients estimated by the UNIFAC group-contribution technique.

Several algorithms were used to solve the steady-state equations with varying degrees of success (Kovach and Seider, 1987b). The algorithms that converged were slow to converge and produced results that did not agree with the experimental data. The results of the initial simulation ($R' = 0.11$, $R'' = 55.0$, $Q_{33} = 4.83$ Mkcal/h, $\Delta T_s = 1.0$) are compared with experimental data in Figure 4. The agreement is quite good except for the bottoms water composition, which shows negligible water in the

Table 3. Heat Capacity Coefficients*

	C_1	C_2	C_3	C_4
		Liquid		
SBA	5.8238E + 01	−2.6650E-01	9.3920E-04	−7.3120E-07
DSBE	1.1021E + 02	−4.3920E-01	1.3630E-03	−1.0737E-06
Water	1.2143E + 01	5.0889E-02	−1.5079E-04	1.5493E-07
MEK	4.0340E + 01	−5.4970E-02	1.7703E-04	−5.5384E-08
Butylenes	3.0534E + 01	−6.6150E-02	1.9130E-04	1.2320E-07
		Vapor		
SBA	1.3740E-00	1.0140E-01	−5.5610E-05	1.1400E-08
DSBE	−8.2177E-00	2.3630E-01	−1.7076E-04	5.1790E-08
Water	8.1015E-00	−7.2000E-04	3.6307E-06	−1.1603E-09
MEK	2.6140E-00	8.5010E-02	−4.5380E-05	9.3620E-09
Butylenes	−7.1500E-01	8.4360E-02	−4.8540E-05	1.0660E-08

*For the polynomial:

$$C_p = C_1 + C_2T + C_3T^2 + C_4T^3, \text{ K, kcal/kmol-K}$$

simulation result (seven orders of magnitude smaller than measured), the temperature difference between trays 31 and 36 (7 K compared with 0.31 K in the simulation), and the decanter temperature. The concentration profiles in Figure 9 confirm that, in the simulation results, water is not present on the bottom 21 trays of the stripping section. Only small changes in concentration are computed and, consequently, just small changes in temperature.

The errors in the total bottoms and overhead (aqueous plus organic product) flow rates are small. The 37 K difference between the simulated and experimental temperatures in the decanter is a consequence of the high amount of butylene in the organic phase. The aqueous and organic product rates and compositions are in excellent agreement, with the exception of the butylene concentration. The flow rates of the organic and aqueous reflux streams agree within 6%. In summary, the simulation results show no water in the stripping section, and consequently do not permit examination of the operator's strategy of adjusting the flow rate of the aqueous reflux to control the temperature difference between trays 31 and 36.

To aid in interpreting the limited temperature and composition data, Figure 10 shows isotherms computed using the coefficients in Tables 5 and 6, at the experimental temperatures in Figure 4. The highest temperature, 381.71 K, is at the SBA vertex. Its saturation pressure, 1.4130 bar, replaces the gauge reading of 1.971 bar, which is apparently in error. Isotherms are plotted at the temperatures and pressures of trays 36, 31, and 2. Note that $P_2 = 1.289$ bar is the experimental gauge reading and P_{31} and P_{36} are estimated using the calculated bottoms pressure, and a pressure drop per tray of 4 in. of water (0.01 bar). In addition, a single vapor-liquid tie line shows the high volatility of water in the stripping section, and the locus of points with

Table 4. Enthalpies at 298 K, kcal/kmol

	Liquid	Vapor
SBA	0	1.2041E + 04
DSBE	0	1.1940E + 04
Water	0	1.0490E + 04
MEK	0	8.3075E + 03
Butylenes	0	4.8055E + 03

$K_{SBA} = K_{DSBE}$ shows the SBA-DSBE azeotrope at 87 mol % SBA.

The curves in Figure 10 place bounds on the temperatures and compositions that are not measured. The liquid composition profile leaves the SBA vertex and passes through the 380.71 K isotherm on tray 36 and the 373.71 K isotherm on tray 31, while remaining to the left of the $K_{SBA} = K_{DSBE}$ line. The compositions in the rectifying section are more difficult to bound because butylene and MEK are present on the top trays. The 359.93 K isotherm, at the conditions of tray 2, lies entirely within the binodal curve. Since an increase of just 5k moves portions of the isotherm outside of the binodal curve, x_2 probably lies near the organic end point of a liquid-liquid tie line (on a butylene- and MEK-free basis).

Returning to the simulations, an attempt was made to extend the water front into the stripping section with the specification $x_{H_2O,33} = 0.01$, but a feasible solution could not be found. Since Magnussen and coworkers (1979) and Prokopakis and coworkers (1981) showed that the steady-state equations for azeotropic towers can possess multiple solutions, an attempt was made to locate improved solutions using a homotopy-continuation method. Success was achieved using the aqueous and organic reflux ratios as parameters in the homotopy algorithm (Kovach and Seider, 1987b).

Initially, the aqueous and organic reflux ratios were set at low values, $R' = 0.05$, $R'' = 10.00$, with $Q_{33} = 4.83$ Mkcal/hr, and $\Delta T_s = 1$ K. The solution, obtained using the homotopy-continuation algorithm, has a single liquid phase on every tray and composition fronts near the bottom of the stripping section, Figure 11, case 1. The mole fraction of water in the bottoms is in close agreement with the experimental measurements, but the concentration of DSBE is too low. To compensate, R'' was increased from 10 to 55. Cases 1–3 in Figure 11 show the gradual movement of the SBA/water composition front up the tower. At $R'' = 30.25$ ($L_1'' = 251.4136$), the front has moved 10 trays up the tower, and when $R'' = 30.30$ ($L_1'' = 251.4159$) the front has reached the feed tray. Then the DSBE composition begins to increase, first in the rectification section, and then gradually throughout the stripping section. Case 4 in Figure 11 shows DSBE in the stripping section at $R'' = 36.60$ ($L_1'' = 252.1837$) and case 1 in Figure 12 presents the solution for $R'' = 55.0$ ($L_1'' = 254.4504$). Note that as R'' increases, the bottoms flow rate

Table 5. Coefficients for Extended Antoine Equation*

	C_1	C_2	C_3	C_4	C_5	C_6
SBA	5.1634E + 1	−1.0587E + 4	0.0000E + 0	−8.5478E-2	6.2124E-5	0
DSBE	1.0607E + 2	−1.6598E + 4	0.0000E + 0	−2.4638E-1	2.1326E-4	0
Water	7.0435E + 1	−7.3627E + 3	0.0000E + 0	6.9521E-3	0.0000E-0	−9.0
MEK	9.9653E + 0	−3.1504E + 3	3.6650E + 1	0.0000E-0	0.0000E-0	0
Butylenes	9.1231E + 0	−2.1324E + 3	−3.3150E + 1	0.0000E-0	0.0000E-0	0

*$\ln\{P\} = C_1 + C_2/(C_3 + T) + C_4T + C_5T^2 + C_6 \ln\{T\}$ (atm, K)

increases and the most significant transition occurs with only a 0.1% change in L_1''.

At this point, the mole fraction of DSBE in the bottoms product is in close agreement with the experimental data, but the water concentration is too low. To increase the water concentration, the aqueous reflux ratio was increased while holding the organic reflux ratio constant. Initially, $R' = 0.05$, $R'' = 55$, with $Q_{33} = 4.83$ Mkcal/hr and $\Delta T_s = 1$ K. Changes in composition are gradual until two liquid phases appear on tray 2 when $R' = 0.12$. When the aqueous reflux ratio increases to 0.1238223, Figure 12, case 2, two liquids are present down to tray 6. A dramatic change occurs as the aqueous reflux ratio is increased by just 0.1% from 0.1238223 to 0.1239933. Two liquid phases move into the stripping section to tray 22 and the SBA/water composition front moves just below tray 22, as shown in Figure 12, case 4. As R' increases further, the fronts move down the tower, building up the composition of water in the bottoms, as shown in Figure 12, case 5. The experimental compositions for the tower are in the vicinity of case 4.

Figure 13 shows excellent agreement between the simulation results for case 3 ($R' = 0.1239506$, $R'' = 55$, $Q_{33} = 4.83$ Mkcal/hr and $\Delta T_s = 1$ K) and the experimental data. Water and DSBE are present in the bottoms stream, the temperatures on trays 2, 31, 36, and 41 match the experimental measurements, and all of the stream flow rates, except for the organic reflux (8% error), are close to the experimental measurements. This close agreement lends support to the composition and temperature profiles in Figure 9, case F, and the flow rate profiles in Figure 14.

The two principal errors are in the composition of the organic phase in the decanter, x_1'', and the flow rate of the organic reflux. The latter is not a major concern because the level controllers in the decanter cause the flow rates of the reflux streams to vary about steady values. However, the high butylene concentration in the decanter leads to a low bubble point temperature, so that there is a 36° temperature difference between the simulated and experimental temperatures. The concentration difference is probably due to a vent on the decanter that permits the butylene to escape. When a withdrawal of butylene from the decanter is specified in a simulation, the decanter composition is in much better agreement with the experimental measurement. This also brings the temperature in line with the experimental measurements.

As the aqueous reflux ratio varies, the homotopy path contains two distinct steady-state solutions over a small range of R', as shown in Figures 4, 9, and 13. The former has just one liquid phase on all of the trays, is easy to obtain using the Newton-based iteration methods, but differs from the experimental data in several key aspects. The latter has two liquid phases on trays 2–20, was obtained only with parameterization using the homotopy-continuation method, and is in excellent agreement with the experimental data. It should be noted that the success of the homotopy-continuation method can be attributed to the small increases in R' as the second liquid phase moves down the column from tray to tray. Parametric studies using the Newton-Raphson method were unable to accomplish this due to singularities in the Jacobian matrix and our inability to manually tune the aqueous reflux ratio. The homotopy parameter permits the continuation method to change variables at limit points, which arise as two liquid phases are introduced on the trays. In this manner, singularities of the Jacobian matrix, which would cause the Newton-Raphson method to fail, are avoided. Details of the homotopy-continuation methods are described by Kovach and Seider (1987b).

Results of the Dynamics Test

The insights gained in the steady-state modeling help to explain the response during the dynamics test, which began at 0810 hours with a 13% decrease in the feed rate from 41.4 to 36.0 gpm (2.6 to 2.27 L/s). The reduction in water decreased

Table 6. Parameters for UNIQUAC Equation

	SBA	DSBE	Water	MEK	Butylenes
			Size/Shape Parameters		
r	3.9235	6.0909	0.9200	3.2479	2.9209
q	3.6640	5.1680	1.4000	2.8760	2.5640
q-prime	4.0643	5.7409	1.6741	2.8760	2.5640
			Interaction coefficients, a_{ij}/R (K)		
SBA	0.0000	−97.2021	213.3998	102.5700	−11.4920
DSBE	209.2880	0.0000	158.6873	182.6900	4.8375
Water	52.2446	1,974.0559	0.0000	−0.0386	379.1000
MEK	−32.5860	−57.2900	468.7700	0.0000	−18.1870
Butylenes	162.6000	3.3576	529.5500	107.7600	0.0000

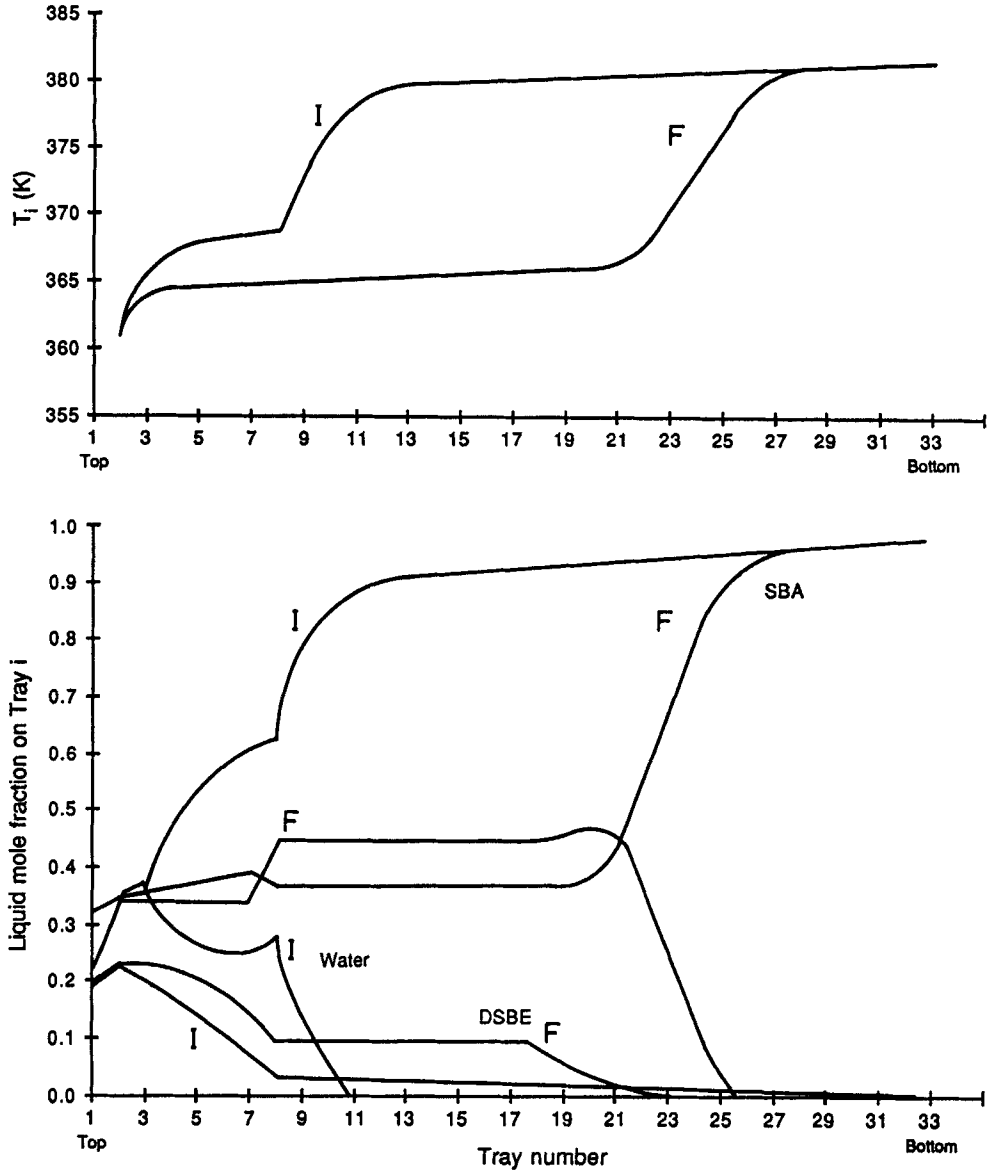

Figure 9. Composition and temperature profiles.
R'' = 55; Q_{33} = 4.83 Mkcal/h; ΔT_s = 1 K.
Case I, initial simulation, R' = 0.12
Case F, final simulation, R' = 0.1239506

the number of trays with two liquid phases, and consequently the composition and temperature fronts moved up the tower with an increase in T_{31}. Anticipating this, the operator increased the aqueous reflux rate, L_1', from 1.6 to 2.8 gpm (0.1 to 0.18 L/s), as shown in Figure 15. Yet, T_{31} increased by 4.5 K to 378.2 K, and hence L_1' was further increased, to a maximum of 3.3 gpm (0.21 L/s) at 0920 hours, when the temperature front had reversed direction and began moving down the tower. L_1' was decreased further to prevent the front from moving too far and then held constant until 1100 hours. Because the aqueous reflux rate was increased to compensate for the decrease in the feed rate, there was no indication of an inverse response as predicted in the dynamic simulations of Prokopakis and Seider (1983b) for the dehydration of ethanol with benzene.

At 1055 hours the level of the organic phase increased, apparently in response to variations in the overhead vapor flow rate. The level controller increased L_1'' from 105 to 117 gpm (6.63 to 7.38 L/s) for approximately 6 min, sending a surge of DSBE down the tower and forming two liquid phases on the trays that previously had concentrations of SBA and water near the binodal curve. With two liquid phases moving down the tower, T_{31} decreased. In response, the operator reduced L_1' by 0.6 gpm. (0.04 L/s). At 1110 hours, the level controller returned L_1'' to 105 gpm (6.63 L/s) and the temperature front reversed direction, moving up the tower. Then, L_1' was returned to 2.6 gpm (0.16 L/s). The net effect of these actions was to move the temperature front up the tower.

At 1153 hours, the feed rate was returned to the pretest level and L_1' was reduced to 1.8 gpm (0.11 L/s). Twenty-two minutes later, at 1215 hours, the level controller increased L_1'' from 102 to

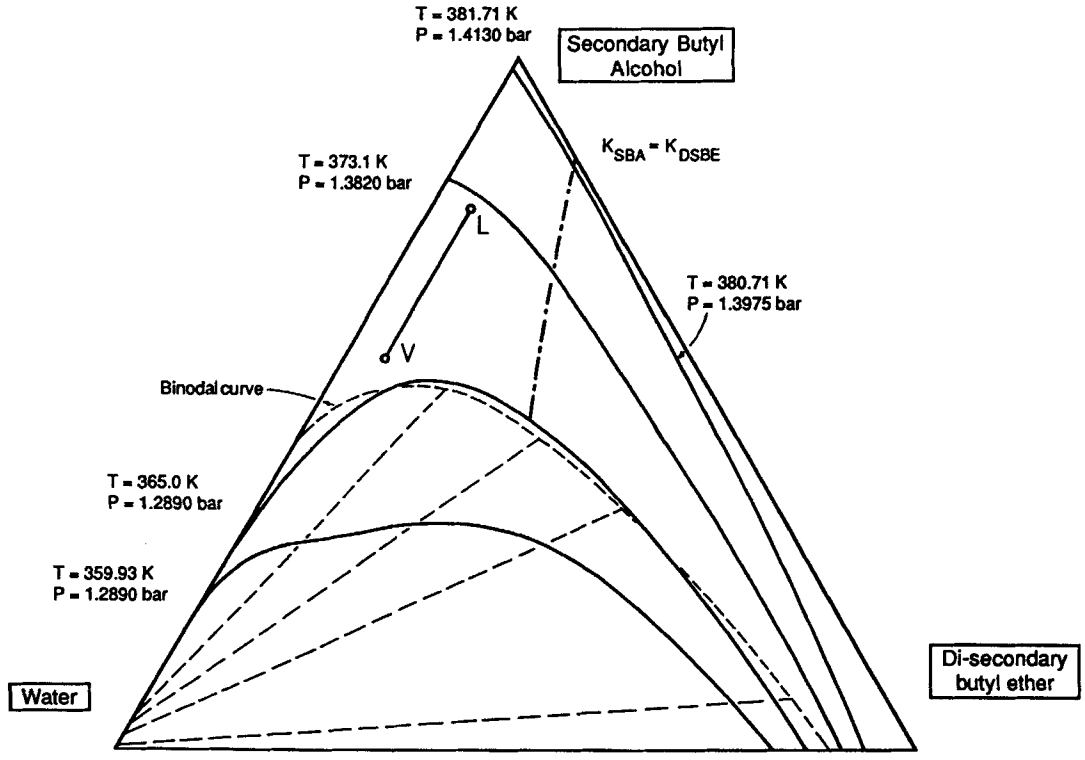

Figure 10. Isotherms for SBA-DSBE-water system at temperature and pressure of trays 2, 31, 36, and 41.
Mole fractions in liquid phase are plotted

133 gpm (6.43 to 8.39 L/s), the overhead temperature, T_2, dropped, and V_2 increased, probably due to flashing of the volatile species in the larger feed stream. The controller maintained L_1'' at this level for approximately 6 min, after which it decreased to 99.7 gpm (6.29 L/s). This time the operator did not adjust L_1' and T_{31} began dropping from 378.2 K at 1220 hours, reached a minimum of 369.8 K at 1225 hours, and returned to 378.7 K by 1240 hours. The drop in temperature lagged 5 min behind the change in L_1''. Fifteen minutes after the pulse of DSBE had passed tray 31, the bottoms temperature, T_{41}, dropped approxi-

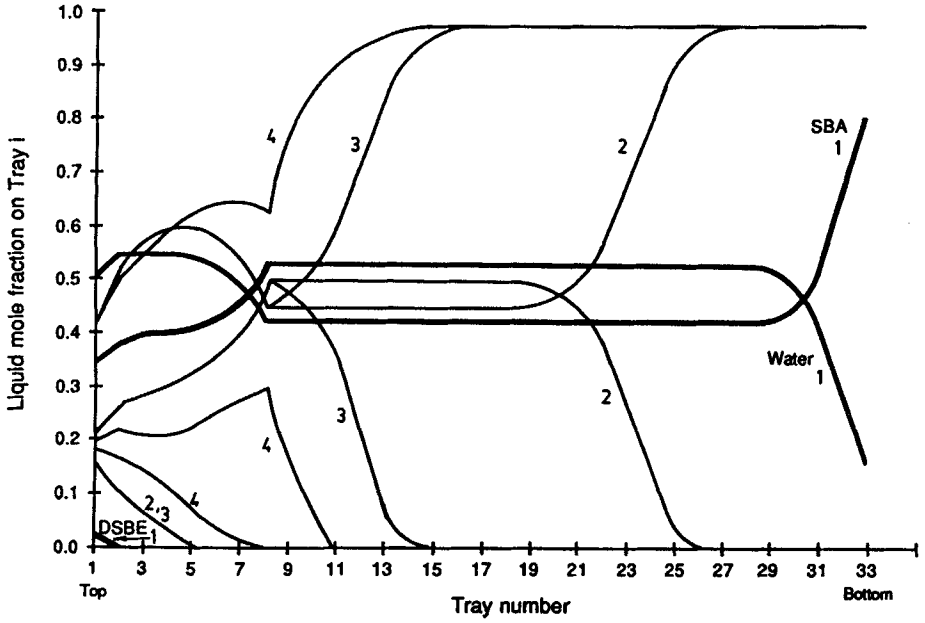

Figure 11. Profiles of liquid mole fractions.
$R' = 0.05$; $Q_{33} = 4.83$ Mkcal/h; $\Delta T_s = 1$ K
$R'' = 10$ (case 1), 30.25 (case 2), 30.30 (case 3), 36.60 (case 4)

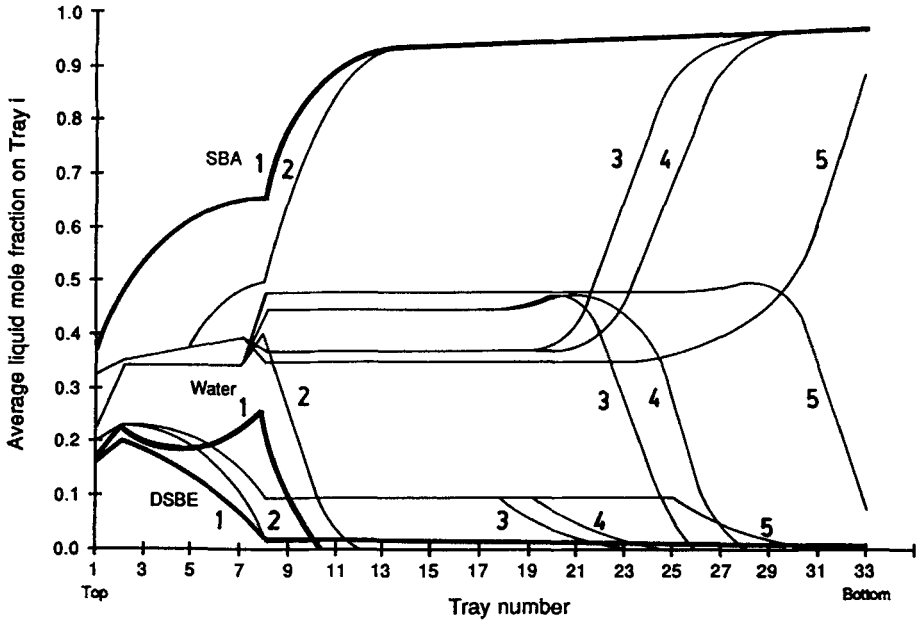

Figure 12. Profiles of liquid mole fractions.
R'' = 55; Q_{33} = 4.83 Mkcal/h; ΔT_s = 1 K
R' = 0.05 (case 1), 0.123822 (case 2), 0.123951 (case 3), 0.123993 (case 4), 0.18 (case 5)

mately 2 K (as the bottoms composition of DSBE was slightly increased in the direction of the minimum boiling SBA-DSBE azeotrope), and remained depressed for about 15 min.

Between 1220 and 1240 hours, L_1'' dropped to 95 gpm (5.99 L/s), probably shortening the response of T_{31} to the increase in L_1'' at 1215 hours. Between 1240 and 1335 hours, L_1'' averaged 103 gpm (6.5 L/s) with short (1–2 min) fluctuations of +15 and −11 gpm (+0.95 and −0.69 L/s), and L_1' was increased from 2.5 to 3.0 gpm (0.16 to 0.19 L/s). At 1335 hours, with all flow rates relatively constant, T_{31} began decreasing. The increase in

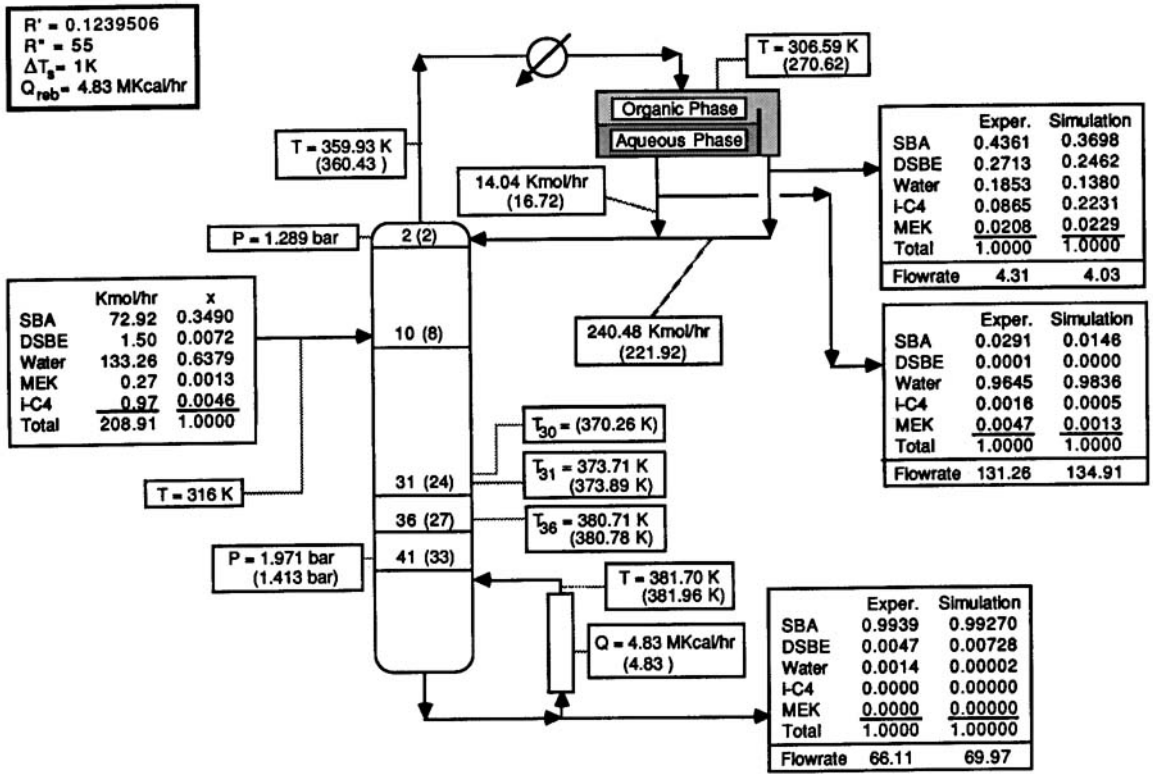

Figure 13. Comparison of simulation results (in parentheses) with experimental data.

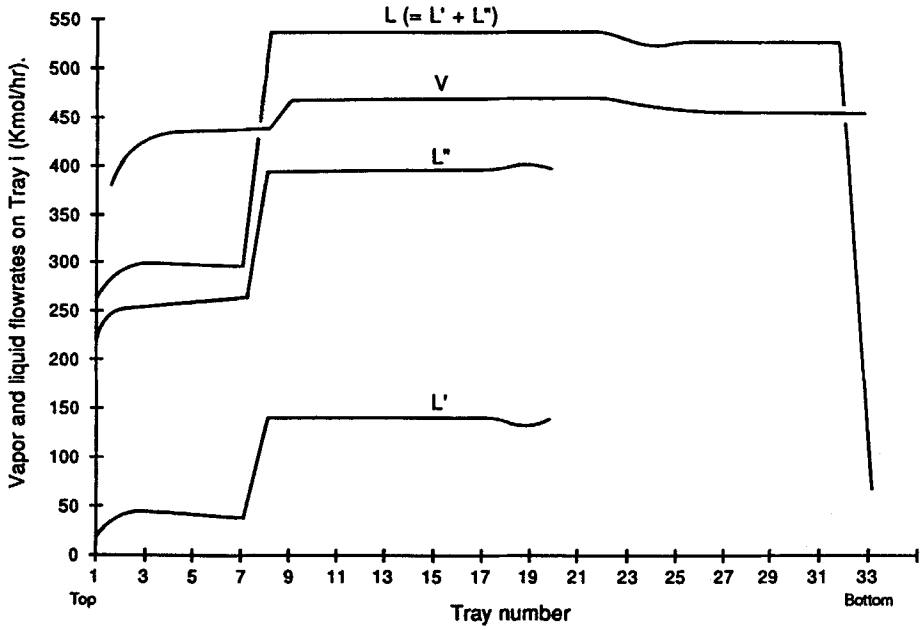

Figure 14. Flow rate profiles for final simulation, case F, Figure 9.

L_1' had moved the two-liquid-phase region down the tower, filling it with water. By the time the operator noted the decrease in T_{31} the tower had accumulated enough water so that the reduction of L_1' had little effect. L_1' was reduced to zero before the temperature front returned to tray 31.

Between 1400 and 1430 hours, the effectiveness of reducing L_1' to control T_{31} was mitigated by entrainment of the aqueous phase in the organic reflux. Table 7 shows evidence of entrainment in that the composition of the organic reflux lies within the binodal curve. The increase of water due to entrainment is 14 kmol/h, which is equivalent to an increase of 1 gpm (0.06 L/s) in L_1'. The organic reflux had dried by 1500 hours and the response of T_{31} to changes in L_1' returned to normal.

Throughout the test, the bottoms product remained on specification. However, the log sheets for the two-week period prior to the test reveal four periods of off-specification operation, as shown in Table 2. In analyzing these data, as in Figure 4, the pressure gauge at the bottom of the tower appears to be in error, and it may be necessary to consider dynamic and nonequilibrium effects. Assuming that the bottoms temperature and composition are correct, the bottoms pressure is corrected. Furthermore, a pressure drop of 0.02 bar between trays 31 and 41 is assumed. Figure 16 shows the T_{31} isotherms and bottoms composition associated with the off-specification periods on Oct. 26, Nov. 2, Oct. 30, and Oct. 29.

Water in the bottoms product on Oct. 26 could have resulted

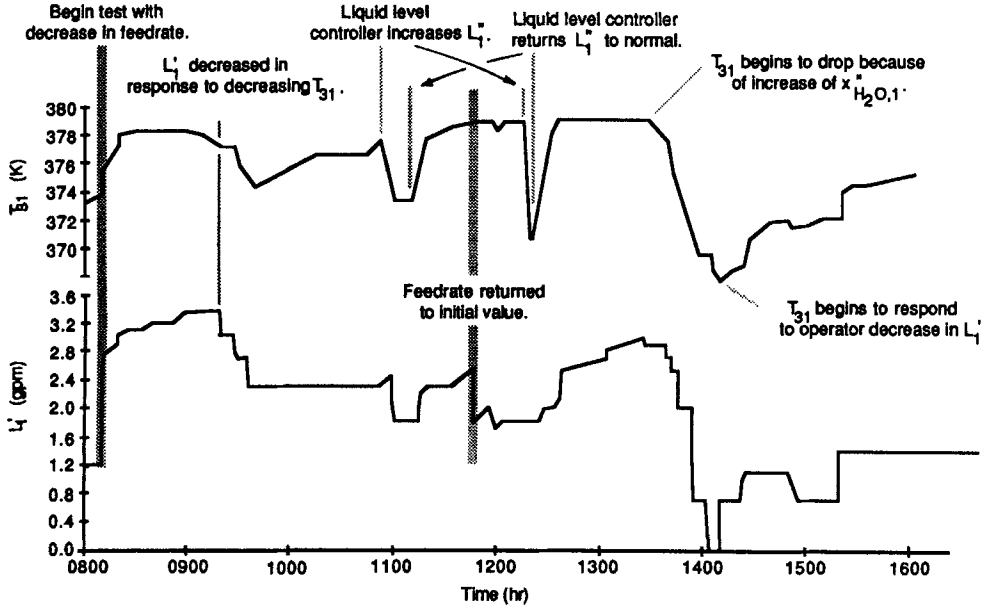

Figure 15. Strip-chart recordings of T_{31} and L_1'.

Table 7. Organic Reflux Composition* During Dynamic Test

	Hour				
	1300	1330	1400	1430**	1500
SBA	44.46	45.76	42.65	38.85	45.21
Water	22.80	21.40	27.70	33.80	22.66
DSBE	23.30	23.49	20.93	19.61	23.05
MEK	1.85	1.87	1.74	1.58	1.88
2-Butene	7.59	7.48	6.98	6.16	7.21
Total	100.00	100.00	100.00	100.00	100.00

*Mole fractions calculated excluding approx. 0.14, 0.03, and 1.00 wt. % of isopropanol, acetone, and unknowns, respectively.
**Approx. 1% of organic reflux sample was entrained aqueous phase.

from insufficient DSBE, excessive water in the reflux, or both. If the aqueous reflux was too high, with sufficient DSBE, two liquid phases would have existed throughout the stripping section. However, the 378.2 K isotherm is outside of the binodal region; consequently, it seems clear that the organic reflux was low. Composition profiles are probably similar to those in Figure 11, case 1. The vapor pressure of the 45/55 mol % mixture of SBA and water, present throughout much of the stripping section, is 1.919 atm, (1.944 bar), which is within the expected error of the calculated P_{31} on Oct. 26.

The analysis of the data for Nov. 2 is more difficult because T_{31} was rapidly decreasing at the time of sampling, varying between 378.2 and 375.2 K. The higher temperature isotherm is plotted, and the lower is approximately the same as that of Oct. 26. For the latter case, the same mechanism as for Oct. 26 can be postulated. However, steady-state simulations have been unable to predict behavior that would explain the former.

The DSBE in the bottoms product on Oct. 29 was probably the result of excessive amounts of aqueous and organic reflux. The T_{31} isotherm is sufficiently near the binodal curve to indicate that two liquid phases were likely in the stripping section. The composition profiles were probably similar to those in Figure 12, case 5, with the DSBE front extending to the bottom tray.

Simulations that compare to the conditions on Oct. 30 have not been found. Examination of the T_{31} isotherm shows that it is not sufficiently close to the binodal region for two liquid phases to exist in the stripping section. However, the water composition in the bottoms suggests that two liquid phases do exist. It suggests that dynamic or nonequilibrium effects must be considered to explain these data.

Conclusions

It is concluded that:

1. The response of the tower to changes in the feed rate and operating variables during the dynamics test are explained with steady-state simulations. When the water entering the tower is increased, either by increasing the feed or the aqueous reflux, the number of trays with two liquid phases is increased and the temperature and composition fronts move down the tower. This is counter to the results of Prokopakis and Seider (1983a,b) for the dehydration of ethanol using benzene (where the specifications were adjusted to permit just one liquid phase on the trays)

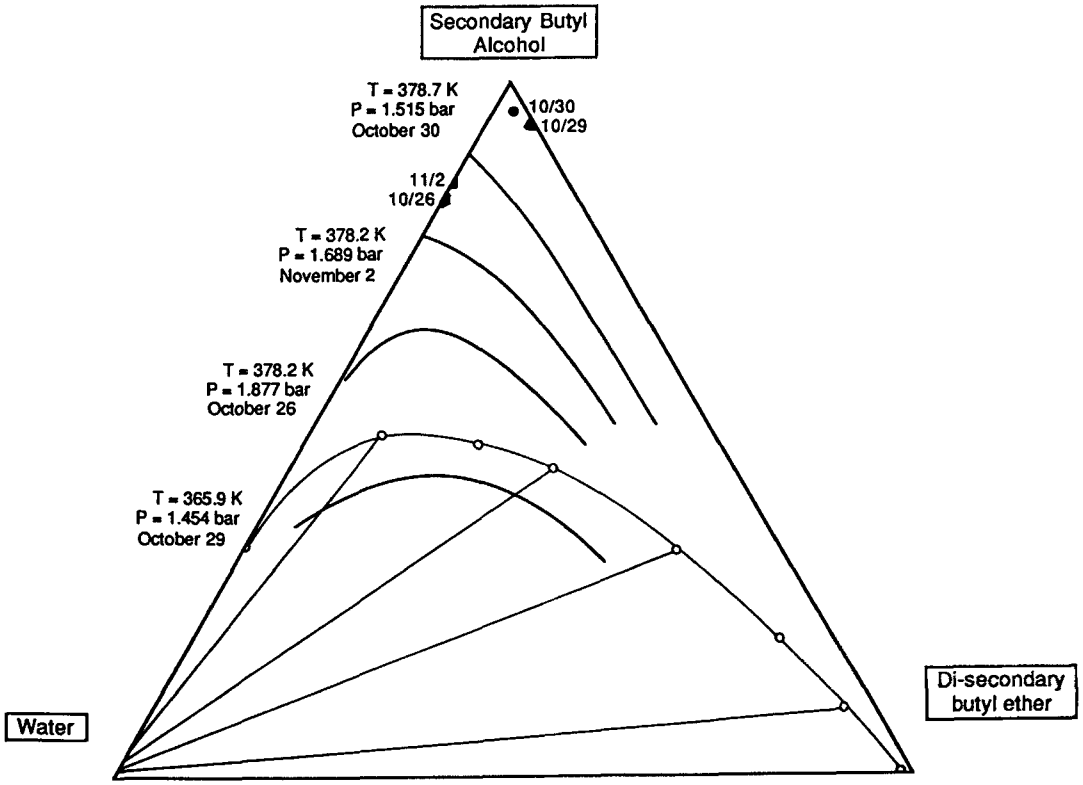

Figure 16. T_{31} isotherms for SBA-DSBE-water system at P_{31}, estimated using an adjusted P_{41}.
Mole fractions in liquid phase are plotted
x_{41} plotted during periods of off-spec operation
° liquid-liquid equilibrium data

and is expected when a tower operates with two liquid phases on its trays.

2. When the entrainer entering the tower is increased, the fronts move down the tower as Prokopakis and Seider predicted. However, the mechanism for the movement is different. For the SBA-DSBE-water system, a small amount of DSBE (3 mol %) significantly decreases the solubility of SBA and water. Thus, when a pulse of DSBE moves down the tower it causes two liquid phases to form. The fronts move down the tower, leaving fewer trays for stripping the entrainer, and consequently the entrainer often contaminates the bottoms product.

3. The location of the fronts is extremely sensitive to the amount of water refluxed to the tower. This is shown in both the experimental data and in computer simulations. Increasing the water in the reflux by 1 mol/h can cause a 9 K decrease in T_{31} as the temperature front moves down the tower. Larger increases of approximately 10 mol/h often occur with small changes in the operating variables when: (a) L'_1 is increased by 1 gpm (0.0631 L/s), (b) the aqueous reflux entrained in the organic phase is increased from 1 to 2%, or (c) $x''_{H_2O,1}$ is increased by 0.03.

4. The homotopy-continuation methods permit the aqueous reflux ratio to be varied over just 0.1% to introduce two liquid phases throughout most of the tower. This can be attributed to the ability of the continuation algorithm to make small increases in the aqueous reflux ratio as the second liquid phase moves down the column from tray to tray. Parametric studies using the Newton-Raphson method were unable to accomplish this due to singularities in the Jacobian matrix and our inability to manually tune the aqueous reflux ratio. The homotopy parameter permits the continuation method to change variables at limit points, which arise as two liquid phases are introduced on the trays. In this manner, singularities of the Jacobian matrix, which would cause the Newton-Raphson method to fail, are avoided.

5. The parameterization with respect to the aqueous reflux ratio resulted in two steady-state solutions over a very narrow range of the reflux ratios, one with a single liquid on the trays, the other with two liquid phases on 70% of the trays. The latter is in close agreement with the experimental data which, to our knowledge, are the first data to be published for an industrial azeotropic distillation tower. Furthermore, the presence of two solutions in such close proximity is consistent with the experimentally observed erratic behavior of the tower.

Acknowledgment

Len Fabiano of the ARCO Chemical Company arranged for these experiments with the SBA II tower and Teddy Tom provided valuable assistance at the plant site. Skip Russell and Kevin Waguespack, the technical service engineers, and the plant operating personnel were very cooperative and helpful during the dynamics test. Partial support was provided by National Science Foundation Project No. CPE-8118023 and is appreciated.

Notation

A_i = flow rate of a side stream from tray i, kmol/s
BP_i = residual of bubble point equation for tray i, kmol/s
d_j = distillate flow rate of species j, kmol/s
D = total distillate flow rate, kmol/s
E_i = residual of energy balance for tray i, kcal/s
EQ_{j1} = residual of constraint equating distillate and reflux mole fractions of species j, kmol//s
f_{ji} = feed flow rate of species j to tray i, kmol/s
F_i = total feed flow rate to tray i, kmol/s
h_i = enthalpy of liquid leaving tray i, kcal/kmol
H_i = enthalpy of vapor leaving tray i, kcal/kmol
$K_{ji} = y_{ji}/x_{ji}$ for species j on tray i
l_{ji} = liquid flow rate of species j leaving tray i, kmol/s
L_i = total liquid flow rate leaving tray i, kmol/s
M_{ji} = residual of a mass balance for species j on tray i, kmol/s
NP_i = number of phases on tray i
N_s = number of chemical species
P_i = pressure on tray i, bar
Q_i = rate of heat transfer to tray i, kcal/s
Q_{ji}^{LL} = residual of a liquid-liquid equilibrium equation for species j on tray i
Q_{ji}^{VL} = residual of a vapor-liquid equilibrium equation for species j on tray i, kmol/s
R = reflux ratio, L/D
S = ratio of a side stream flow rate to flow rate of remaining stream
SP = residual of a specification equation
T = temperature, K
v_{ji} = vapor flow rate of species j leaving tray i, kmol/s
V_i = total vapor flow rate leaving tray i, kmol/s
x'_{ji} = mole fraction of species j in first liquid phase leaving tray i
x''_{ji} = mole fraction of species j in second liquid phase leaving tray i
y_{ji} = vapor mole fraction of species j in vapor leaving tray i
ΔT_s = degrees of subcooling in the condenser/decanter, K
γ_{ji} = activity coefficient of species j on tray i

Subscripts

i = tray index
j = species index

Superscripts

F = feed
L = liquid phase index
v = vapor phase
$'$ = first liquid phase
$''$ = second liquid phase

Literature cited

Ferraris, G. B., and M. Morbidelli, "Mathematical Modeling of Multistaged Separators with Mixtures Whose Components Have Largely Different Volatilities," *Comp. Chem. Eng.*, **6**, 4, 303 (1982).

Kovach III, J. W., *Heterogeneous Azeotropic Distillation—An Experimental and Theoretical Study*, Ph.D. Thesis, Univ. Pennsylvania, 1986.

Kovach III, J. W., and W. D. Seider, "Vapor-Liquid and Liquid-Liquid Equilibria for the System Sec-butanol, Disecbutylether, Water," submitted to *J. Chem. Eng. Data*, 1987a.

———, "Heterogeneous Azeotropic Distillation—Homotopy-Continuation Methods," accepted by *Comp. Chem. Eng.* (1987b).

Magnussen, T., M. L. Michelsen, and A. Fredenslund, "Azeotropic Distillation Using UNIFAC," *Inst. Chem. Eng. Symp. Ser.*, No. 56, 3rd Int. Symp. Distillation, ICE, Rugby, Warwickshire, England (1979).

Napthali, L. M., "The Distillation Column as a Large System," preprint, AIChE Ann. Meet. San Francisco (1965).

Napthali, L. M., and D. P. Sandholm, "Multicomponent Separation Calculations by Linearization," *AIChE J.*, **17**, 148 (1971).

Prokopakis, G. J., B. A. Ross, and W. D. Seider, "Azeotropic Distillation Towers with Two Liquid Phases," *Foundations of Computer-aided Chemical Process Design*, R. S. H. Mah and W. D. Seider, eds. AIChE, New York (1981).

Prokopakis, G. J. and W. D. Seider, "Feasible Specifications in Azeotropic Distillation," *AIChE J.*, **29**, 1 (1983a).

———, "Dynamic Simulation of Azeotropic Distillation Towers," *AIChE J.*, **29**, 1017 (1983b).

Robinson, C. S. and E. R. Gilliland, "Elements of Fractional Distillation," McGraw Hill, NY, 312 (1950).

Ross, B. A. and W. D. Seider, "Simulation of Three-Phase Distillation Towers," *Comp. Chem. Eng.*, **5**, 1 (1980).

Schuil, J. A., private communication (1984).

Wayburn, T. L., and J. D. Seader, "Solution of Systems of Interlinked Distillation Columns by Differential Homotopy-Continuation Methods," *Foundations of Computer-aided Chemical Process Design*, A. W. Westerberg and H. H. Chien, eds. CACHE (1984).

Manuscript received Sept. 4, 1986, and revision received Feb. 6, 1987.